NASA CR-137733

VECTORED THRUST INDUCED LIFT EFFECTS FOR SEVERAL EJECTOR EXHAUST LOCATIONS ON A V/STOL WIND TUNNEL MODEL AT FORWARD SPEED

Prepared by

A. D. Sharon

August 1975

Prepared under Contract NAS2-8864
By Los Angeles Aircraft Division
ROCKWELL INTERNATIONAL CORPORATION
Los Angeles, California
For
AMES RESEARCH CENTER
NATIONAL AERONAUTICS AND SPACE ADMINISTRATION

SUMMARY

The results and analysis of aerodynamic force data obtained from a small scale model of a V/STOL research vehicle in the R.I. Low Speed Wind Tunnel (NAAL) are presented. The analysis of the data includes the evaluation of aerodynamic-propulsive lift performance when operating twin ejector nozzles with thrust deflected. Three different types of thrust deflector systems were examined: 90° downward deflected nozzle, 90° slotted nozzle with boundary layer control, and an externally blown flap configuration. Several nozzle locations were tested, including over and underwing positions. The interference lift of the nacelle and model due to jet exhaust thrust is compared and results show that 90° turned nozzles located over the wing (near the trailing edge) produce the largest interference lift increment for an untrimmed aircraft, and that the slotted nozzle located under the wing near the trailing edge (in conjunction with a BLC flap) gives a comparable interference lift in the trimmed condition. The externally blown flap nozzle produced the least interference lift and significantly less total lift due to jet thrust effects.

INTRODUCTION

A wind tunnel test program using a full span model of a V/STOL aircraft was tested in order to provide consistent data regarding interference lift between deflected nozzle exhausts and the model wing when the nozzles are located at various positions.

Some evidence that certain locations of the nozzles with respect to the flap trailing edge are beneficial was found for small nozzles from previous test results published in the literature. It is believed that large lift increases shown for aft nozzle locations are due to entrainment of flow into the exhaust flow, the mechanism involving a flow velocity increase at the upper flap and wing surfaces.

For design optimization a question unanswered was where to locate the twin exhausts with respect to the wing to obtain a high lifting capability. Aerodynamically, the location on the wing is not so much a concern for the hover condition as it is for conditions at low forward speeds, such as encountered during STOL operations. Even when the primary requirements of an aircraft may be a hover capability, it will operate in the STOL mode during overweight conditions.

The location of the exhausts has a considerable impact. Reference 2 shows the effect of exhaust location on measured induced wing lift, excluding the forces on the nacelle. Summary plots derived from this reference are presented here in figure 1 and 2. A similar plot is given in reference 3. It is seen that a forward location results in a negative interference lift, whereas an aft location results in a positive interference. The same trend is found in reference 4 where measured model interference lift is presented at fore and aft nacelle locations, each together with the wing as a unit. Data derived from this reference are given in figure 3, showing a somewhat more severe lift loss. Figure 4 shows that the trend exists both flaps up and down, and at various angles of attack for speeds up to and beyond $V_\infty / V_j = 0.4$ (V_∞ = aircraft speed, V_j = jet exhaust velocity).

Reference 5 indicates also a strong effect of the vertical location: a 33% lift loss for the exhaust located below the wing, and a 75% lift gain above the wing, with both positioned in an aft location behind the wing. The information thus far obtained pertains to various different wind tunnel models and different test setups which may introduce unknown variables from one test to another. For example, the fan inlets of the tests of reference 5 were located near the 40% chord station of the wing, whereas the others had inlets ahead of the wing or none at all. In order to compare various locations on a consistent basis it was desired to conduct a wind tunnel test simulating various exhaust locations, by using consistent model components.

Exhausts are located at various positions under the wing and compared with one over the wing, and all inlets are located ahead of the wing. Exhausts simulated are fairly large, representing fans with high bypass ratios.

Other means to increase the induced lift were also tried. These involved bringing high exhaust velocities as close to the flap trailing edges as possible so that the entrainment effect may be increased. This may be achieved by opening slots in the exhaust duct. A simple large chord flap with leading edge boundary layer control behind the thrust deflector is combined with an opening of the deflector upper aft side (slots) so that the fan exhaust will fill in the region between the deflector and the flap.

An alternate means of providing power-induced lift during STOL operation was tested using externally blown flaps. Unlike the previously discussed nozzles, the ejector thrust is deflected directly onto the wing flaps rather than turning the jet flow via nozzle exhaust rotation. The externally blown flap is included so as to provide a consistent comparison with the deflected nozzle thrust. Figure 5 shows the general location of the various nozzles tested relative to the model wing.

The preliminary results and conclusions of this report, less the externally blown flap results, are also presented in reference 6.

LIST OF SYMBOLS

BLC	Boundary layer control
c, c_w	Local wing chord, cm (in.)
C_L	Lift coefficient
C_P	Pressure coefficient
D	Width of basic nacelle = constant = 20.3 cm (8 in) square
EBF	Externally blown flap
L	Total lift, Newtons (lbs)
$\frac{\Delta L}{T}$	Ratio of change in lift due to power at forward velocity to reference thrust for all nozzles aft of wing leading edge
$\left(\frac{\Delta L}{T}\right)_F$	Ratio of change in lift due to power at forward velocity to reference thrust for trim nozzle forward of wing leading edge
MAC, $\bar{c}$	Mean aerodynamic chord
q	Wind tunnel dynamic pressure, $\frac{\text{Newtons}}{m^2}\left(\frac{\text{lbs}}{ft^2}\right)$
S_{REF}	Wing reference area, m^2 (ft^2)
T	Reference thrust, Newtons (lbs)
ΔT_q	Thrust increment at forward velocity, Newtons (lbs)
$\frac{V_\infty}{V_j}$	Speed ratio
WFM	Primary nozzle weight flow, $\frac{\text{Newton}}{\text{sec}}\left(\frac{\text{lbs}}{\text{sec}}\right)$
X/C	Exhaust location behind wing leading edge
$\frac{y}{b/2}$	Wing spanwise station

LIST OF SYMBOLS (Concluded)

Z/C	Vertical thrust location
α	Angle of attack, deg.
δ_F	Flap deflection, deg.
δ_N	Thrust nozzle deflection, deg.

MODEL DESCRIPTION AND INSTALLATION

The model is a .13 scale R.T. model of the Sabreliner aircraft modified to a high wing location adjacent to which large ejector nacelles are located. Flow through the twin nacelles is simulated by high pressure air piped to the front of the nacelles as shown in figure 6. The rear portion of the nacelles are interchangeable which allows one to test various thrust deflector configurations without altering the forward portion of the nacelle.

The model forces and the nacelle forces are each measured by separate balances to provide the mutual interference effects. The model utilizes the tunnel planar balance while the nacelle (left only) uses a movable 6.35cm (2.5 in.) diameter internal strain gage balance.

Mass flow through the nacelles is measured by a flow rake containing 12 static pressure and 21 total pressure orifices in each nacelle. These readings should aid in isolating the weight flow and thrust produced by the blowing of the primary (shop air) and secondary (induced tunnel air) flow.

Model planform with nacelles in the forward position (deflected thrust centerline at $\bar{c}/4$) is shown in figure 7. Two different flaps are used, generally a 60° double slotted flap, and in one case a large chord 90° single slotted flap with a vane, see figure 8. The large flap angle is used only over a portion of the flap span where the ejectors will be located. No wing leading edge devices are installed.

The "basic" ejector has a single exhaust, being 20.3cm (8 inches) square, whereas the slotted nozzle has exhausts at a number of locations. The slotted nozzle is used only in conjunction with the large chord 90° single slotted flap. The upper exhaust location is very narrow and feeds air to the vane of the flap to simulate boundary layer control. There are three additional narrow exhaust slots on the ejector housing further down on the rear side. These are used to energize and entrain air flowing over the wing and along the upper surface of the flap (see figure 9). The total exhaust area of this ejector is equal to the basic ejector, i.e., 413cm^2 (64 in.^{2}), but the main exhaust, pointed downward, has only 78.8% of this area. The idea behind the slotted ejector and the single slotted 90° flap is to be able to locate the engine exhaust relatively far forward under the wing for VTOL balance reasons, and, simultaneously to avoid a large distance between the engine exhaust pipe and the flap trailing edge.

The externally blown flap nozzle, also shown in figure 9, is merely a 20.3cm (8 in.) square flat plate attached to the bottom of the nacelle and angled 25° upward from the horizontal.

Photographs of the model alone and model and ejector installation in the NAAL facility are shown in figure 10. The ejector was located at various longitudinal stations under the wing, each with a small vertical clearance with respect to the lower wing surface so that the forces on the wings and the nacelles could be measured separately. The forward position, located longitudinally at the 1/4 chord station of the MAC, is shown in the photograph in figure 11a. The ejectors located above the wing, shown in figure 11b, were located longitudinally such that the exhaust would just barely avoid the last flap segment. A filter block was installed on the upper surface just ahead of the flap shroud to prevent premature lateral inflow from air on the upper wing surface into the exhaust. Generally, the main model had to be inclined to a small angle of attack to provide the proper clearance between ejectors and the model, whereas the ejectors were always parallel to the tunnel wall.

The slotted BLC nozzle and the externally blown flap nozzle are shown in figures 12a and b, respectively. Detailed model description, instrumentation, data reduction, and tunnel installation is presented in reference 7.

TEST CONDITIONS

Test conditions for the V/STOL model in the NAAL facility ranged from q = 0 to 958 Newton/m^2 (20 lbs/ft^2). The nominal Mach number at q = 958 N/m^2 (20 lbs/ft^2) is .12 or the equivalent airflow velocity is 40.8 meters/sec (134 ft/sec) and a corresponding Reynolds number is .85 x 10^6/ft. The primary and secondary air flow was set in the tunnel as a function of the static pressures and total pressure ratio at the rake and calibrated versus tunnel freestream pressures.

DISCUSSION

Of primary importance in the analysis of ejector nozzle performance is the determination of actual nozzle thrust due to jet nozzle air flow through the nacelle. This reference thrust value can then be used to isolate the aerodynamic induced lift due to power as well as provide a means of comparing the various ejector nozzles to each other (by non-dimensionalizing them by exhaust thrust). Although the exhaust thrust may have been determined by weight flow calculations using static and total pressures measured at the rake, data reduction techniques used proved too inaccurate to serve as a reliable thrust. The velocity profile at the rake varied from Mach = .16 near the nacelle wall to Mach =.63 in the center of the rake at maximum primary jet weight flow. This large change creates difficulty in calculating accurate weight flows (primary + secondary) without precise integration of pressure data, rather than the averaging technique used in the present data reduction. Other factors such as possible compressibility effects and loss of momentum around the 90° bend (resulting in possible boundary layer build-up near the exhaust) are unknown and may distort the true nozzle weight flow and velocity measurement. Therefore, only the force balance data was used in the analysis to arrive at lift and thrust values. Table I summarizes the model and nacelle lift balance data that is used in this analysis.

To obtain the reference thrust, the entrainment interference force of the flow on the external walls of the nacelle alone must be determined. This was done by installing an entrainment shield at static tunnel condition and jet power through the ejector. The shield is a board placed flat against the exhaust face such that only the nozzle exhaust fits through. It is supported by the tunnel floor and merely acts in preventing possible aerodynamic forces due to exhaust flow forming on the outside of the nozzle. The data, however, did not reveal any entrainment lift for either the basic nozzle or the slotted (BLC) nozzle at q=0. Therefore, the thrust at q=0 is the power-on lift=756N (170 lbs) for the basic nozzle alone. At forward speed additional flow enters the nacelle and becomes part of the reference thrust. This thrust (ΔTq) was estimated to be about 80N (18 lbs) (nacelle frontal area times dynamic pressure). This is also verified by nacelle balance lift forces at forward speed with power off. The question of possible secondary flow due to forward velocity through the nacelles can be resolved by examining the measured weight flow and velocity increments at the rake. Although these calculated values were determined to be too inaccurate for absolute thrust levels (discussed previously), the incremental weight flow and velocity between static and forward speed with power on is a close approximation of the thrust due to forward speed. The rake data show increment ranges from 14 to 23 lbs and can be interpreted to indicate no significant secondary flow due to tunnel velocity. The thrust of the ejector nozzle at q=958N/m^2 (20 lbs/ft^2) is the total lift minus all

aerodynamic lift, i.e., no entrainment is included in the thrust. Figure 13a illustrates the component forces such that the entrainment force can be isolated. The reference thrust is therefore thrust due to jet flow plus added thrust due to forward speed or 836N (188 lbs).

In the present report the increase of lift due to power effects with free stream dynamic pressure is considered to be an entrainment effect and is not considered part of the reference thrust of the nacelle. An earlier analysis (reference 6) assumed that this increase was due to a more efficient ejector nozzle operation and added this increase to the basic thrust, rather than consider it an aerodynamic interference force. When an analysis (such as the present one) is made using different types of ejectors at varied locations, there is no assurance that such entrainment (or a smaller portion) would exist. When the ejector nozzles are moved to their location with respect to the wing, the change in lift due to power at forward speed creates other aerodynamic interference lifts. As an example, figure 13b presents a graphic representation of this interference lift for the aft position underwing nozzle. It is constructed very much the same as the figure above it, except that the total sum of the model plus nacelle balance lift data (in each others presence) was used. Some nozzle entrainment effects, previously mentioned, might exist within the interference lift, but this cannot be presently determined.

The underwing location of the basic nacelles in the presence of the wing and body exhibits a relatively high lifting force of approximately 1378N (310 lbs) with power on, as shown in figure 14. Comparison with the 1156N (260 lbs) for the nacelles alone (figure 13a) points toward a suction force on the rear upper surface of the nacelles generated by the presence of the wing. This is sketched in figure 15. Evidence of the existence of such a region of negative pressures was obtained from measurements in reference 1, and pertinent pressure distributions from this reference are reproduced here in figure 16. This figure shows the pressures on the lower surface of the wing behind the centerline of the thrust exhaust, as well as immediately outboard of the nacelles. The effect of power application on these pressures is shown.

The lift on the overwing nacelles (figure 14) is much less, having no such negative pressure field. As a result, the power effect on this nacelle is relatively low. Likewise, the lift of the slotted (BLC) nozzle shows a large drop in nacelle lift, but this is due primarily to the presence of a boundary layer control device over the wing flap. Their potential benefit will be felt on the flap and wing surfaces. Analysis of the externally blown flap nozzle requires somewhat different conceptual treatment in this figure since the flow is turned upward and potentially favorable lift is derived from positive (rather than negative) pressure under the wing and increased circulation over the wing flap. As expected, the nozzle experiences a negative lift of -179N (-41 lbs) due to the downward component of

lift on the nozzle flap. However, when examining the force data for the model in the presence of the nacelle, in figure 17, the externally blown flap nozzle shows a much larger incremental lift due to power than any of the other ejector types tested. This can be attributed entirely to the fact that all the thrust is deflected upward towards the wing flaps. The deflected thrust is just able to produce as much added lift to the wing as the reference thrust level.

Power effects on the underwing nacelle (also shown in figure 17) tend to increase as the nozzle is moved aft. This may be due to greater negative pressures from increased wing circulation over the upper part of the wing. The overwing nozzle displays the largest lift increase due to power among the turned exhaust nozzles benefiting from increased circulation over the upper surface of the wing. The slotted (BLC) nozzle produces higher wing lift increments than the underwing nozzle (located at the same chordwise location) due to increased circulation due to the BLC over the single flap. The BLC device keeps the flow attached to 90° deflection angle and was verified dur the test with a flow probe.

It should be noted that comparison of lift values may be misleading since the wing was placed at different angles of attack relative to the nacelle. Observation of the wing and body in the presence of the nacelle did not show much difference in lift between $\alpha = 4°$ and 8°, power-on and off. This may be due in part to unfavorable interference effects on the wing from the large nacelle. Figure 18 presents the lift coefficient of the model alone in which a 45 lbs difference in lift exits between $\alpha = 4°$ and 8° and confirms the above conclusions. Therefore, incremental lift differences due to power are more meaningful in comparing nozzle performance than absolute lift.

The total lift (the balance lift force of the model plus the lift force of the two nacelles, each in each others presence) is presented in figure 19. The results tend to follow previously established trends: the overwing nozzle shows the largest lift gain and aft movement of the basic underwing nozzle produces increased lift increment. The slotted nozzle shows a comparable lift increment due to power to the underwing nozzles. The externally blown flap nozzle not only shows a small total lift gain due to power effects, but the overall total lift falls far short of lift values for the other nacelles (taking into account angle of attack differences). This is primarily caused by a negative lift component on the deflector, rather than a positive lift increment shown for the other nozzles. In the present case the ejector exit is large in comparison to the wing flap and a large deflection angle is needed to immerse the whole wing flap in the exhaust. Also, note that the exhaust is turned much less than 90°, the flap being deflected only 60°.

Interference lift due to power is the additional lift due to the mutual presence of the model and nacelle at forward velocity of $q = 958 N/m^2$ ($20 lbs/ft^2$). It is determined by isolating power effects and forward effects as previously discussed in figure 13b. This eliminates all non-interference aerodynamic forces and reference thrust, which leaves only the change in lift due to power. A comparison of this interference lift reveals that the largest lift change occurs for the overwing nacelle, as shown in figure 20. The externally blown flap, on the other hand, shows the poorest induced lift. Although precise explanation is difficult in assessing the EBF performance for one location and one flap setting, the use of the flap to deflect nozzle exhaust flow creates negative lift due to power on the nacelle and thereby reduces the total net lift when the power is on.

Positive lift interference exists for all ejector nozzle configurations and these results show that the trend in lift agrees with results given in figures 1 and 2 for the underwing nacelle, perhaps somewhat better. This might be in part due to a large flap deflection or the use of double slotted flaps. The determination of reference exhaust thrust might also distort the magnitude of the $\Delta L/T$ values, somewhat, since small changes in reference thrust produce large changes in $\Delta L/T$. However, comparison between ejector nozzles matches previous data very closely.

It should be noted that although the overwing concept provides the greatest amount of interference lift, the problem of trimming the aircraft reduces the potential benefits considerably. If a third thrust nozzle is used at a distance of 100% forward of the local wing leading edge to balance the aircraft about the .63 C_W (approximate location of center of lift for the model alone, flaps down), the interference lift results are changed significantly.

One way of including trim effects on interference lift is to assume that the interference lift contributes little to the moment. Test results show that center of pressure varies from (x/c) = .46 for the aft underwing nozzle to .90 for the overwing body, with most falling in .50 and .60 region. Furthermore, aerodynamic balancing with conventional control surfaces is neglected, as well as the incremental pitching moment due to jet thrust effects on the wing flap. The overall interference lift then becomes

$$\left(\frac{\Delta L}{T}\right)_{TRIM} = \left(\frac{\Delta L}{T}\right)_F \cdot \frac{T_F}{T} + \left(\frac{\Delta L}{T}\right) \cdot \left(1 - \frac{T_F}{T}\right)$$

where $(\Delta L/T)$ is taken from figure 21, $(\Delta L/T)_F = -0.25$ is taken from figure 1.

Balancing about 63% local chord requires a ratio of front exhaust to aft nozzle of $T_F/T = (\ell/c_W)/1.63$, where ℓ/c_W = distance from .63c to thrust axis

centerline. The above equation holds only for nozzles where the thrust axis line is behind the .63c line and requires a positive lift from a forward nozzle. Trimmed lift increment results are presented in figure 21. Neither the slotted nozzle or the externally blown flap nozzle are significantly effected by any trim requirements. However, the overwing nozzle loses much of its favorable interference lift. The slotted BLC nozzle appears to show the most promise, indicating that a great deal depends upon the thrust moment arm (as well as the untrimmed interference lift). The externally blown flap nozzle results are not effected since the assumed thrust line is very close to the moment reference.

CONCLUSIONS

1. Of the three distinct ejector nozzle types, the largest in positive lift due to jet exhaust power (interference lift) occurs using the basic nozzle in the overwing position. The overwing nozzle fully utilizes jet flow over the upper surface of the wing to increase circulation while the slotted (BLC) nozzle only uses a small portion of the thrust for this purpose, via boundary layer control. The externally blown flap nozzle increases wing lift circulation much more than any of the others, but since all the nozzle jet flow is deflected upward toward the wing flap, the nozzle creates a negative lift contribution to the net total lift.

2. Aft movement of the basic underwing nozzle increases positive interference lift, indicating greater lift interference increment due to increased wing circulation.

3. Lift interference results can be significantly effected by trim requirements. If an additional nozzle is added for trim purposes, the extracted thrust reduces potential lift interference. Therefore, the larger the thrust moment arm, the less lift interference. Results using a forward trim jet nozzle indicate that the slotted (BLC) nozzle produces the largest positive lift interference. The lift interference differences between the various nozzles, however, become much smaller in the trimmed than in the untrimmed condition.

4. The externally blown flap nozzle, though a much more simplistic concept in its application, provides little in the way of aerodynamic lift enhancement at 60° flap angle, in comparison to 90° deflected nozzles at low forward speeds. Total lift capability, power on, compares very unfavorably with all other nozzles tested.

REFERENCES

1. Mineck, R. E., and Margason, R. J., "Pressure Distribution on a Vectored-Thrust V/STOL Fighter in the Transition-Speed Range," NASA TM X-2867, March 1974.

2. Carter, A. W., "Effects of Jet Exhaust Location on the Longitudinal Aerodynamic Characteristics of a Jet V/STOL Model," NASA TN D-5333, July 1969.

3. Margason, R. J., "Review of Propulsion-Induced Effects on Aerodynamics of Jet/STOL Aircraft," NASA TN D-5617, February 1970.

4. Mineck, R. E., and Schwendemann, M. F., "Aerodynamic Characteristics of a Vectored-Thrust V/STOL Fighter in the Transition-Speed Range," NASA TN D-7191, May 1973.

5. Novak, L. R., "The Lift/Cruise Fan Multimission V/STOL Aircraft," AIAA Paper 75-277, February 1975.

6. Renselaer, D. J., "Effects of Fan Exhaust on Aerodynamic Characteristics of a Twin Lift Fan Aircraft in the STOL Mode," Rockwell International, NA-75-498. Paper presented at the Naval Air Systems Command's Workshop on Prediction Methods for Jet V/STOL Propulsion Aerodynamics, July 28 - 31, 1975.

7. Stone, G. M., "Pretest Information for Investigation of Pressure System Interference Effects on Wing Lift Characteristics, Multimission V/STOL Configuration," Rockwell International, NA-75-340.

TABLE I. MODEL AND NOZZLE BALANCE DATA

CONFIG.	RUN	q (NEWTON/m²)	q (LB/FT²)	WFM (NEWTON/SEC)	WFM (LB/SEC)	α (DEG)	LIFT MODEL (NEWTON)	LIFT MODEL (LB)	LIFT NOZZLE (NEWTON)	LIFT NOZZLE (LB)	LIFT TOTAL (NEWTON)	LIFT TOTAL (LB)
BASE NOZZLE ALONE	16	0	0	16.2	3.65	—	—	—	756.5	170	756.5	170
	14	958	20	16.1	3.61	—	—	—	1157.	260	1157.	260
	13	958	20	0.	0.	—	—	—	298.2	67	298.2	67
MODEL ALONE	47	958	20	—	—	0	1037.	233.	—	—	1037.	233
	↓	↓	↓	—	—	4	1237.	278.	—	—	1237.	278
				--	—	8	1442.	324.	—	—	1442.	324
FORWARD UNDERWING NOZZLE	18	0	0	16.4	3.68	4	-17.8	-4.	765.4	172	747.6	168
	20	958	20	16.5	3.71	↓	1086	244.	1193.	268	2278.	512
	19	958	20	0.	0.	↓	1086	244.	289.3	65	1375.	309
MID UNDERWING NOZZLE	23	958	20	16.3	3.66	4	1224.	275.	1175.	264	2399.	539
	22	958	20	0.	0.	4	1126.	253.	271.5	61	1397.	314
	31	0	0	16.3	3.66	8	-17.8	-4.	752.1	169	734.3	165
	29	958	20	16.1	3.62	↓	1259.	283.	1126.	253	2385.	536
	28	958	20	0.	0.	↓	1130.	254.	267.	60	1397.	314
AFT UNDERWING NOZZLE	—	0	0	16.0	3.60	8	-17.8	-4.	752.1	169	734.5	165
	26	958	20	16.0	3.60	↓	1513.	340.	1019.	229	2532.	569
	25	958	20	0.	0.	↓	1259.	283.	182.5	41	1442.	324

TABLE I (CONTINUED). MODEL AND NOZZLE BALANCE DATA

CONFIG.	RUN	q		WFM		α	LIFT					
							MODEL		NOZZLE		TOTAL	
		(NEWTON/m²)	(LB/FT²)	(NEWTON/SEC)	(LB/SEC)	(DEG.)	(NEWTON)	(LB.)	(NEWTON)	(LB.)	(NEWTON)	(LB.)
OVER WING NOZZLE	46	0	0	16.3	3.66	0	-25.4	-5.7	761.	171	734.3	165
	44	958	20	15.9	3.58	↓	1589.	357	1032.	232	2617.	588
	43	958	20	0.	0.	↓	912.2	205	280.4	63	1193.	268
SLOTTED NOZZLE ALONE	3	0	0	16.5	3.70	—	—	—	703.1	158	703.1	158
	5	958	20	15.9	3.58	—	—	—	930.1	209	930.1	209
	6	958	20	0.	0.	—	—	—	149.1	33.5	149.1	33.5
SLOTTED NOZZLE	42	0	0	16.5	3.70	0	27.1	6.1	685.3	154	712.	160
	40	958	20	15.7	3.54	↓	1344.	302	883.3	198.5	2227.	500.5
	39	958	20	0.	0.	↓	1077.	242	120.2	27	1197.	269
BLOWN FLAP NOZZLE ALONE	10	0	0	16.1	3.62	—	—	—	-182.5	-41	-182.5	-41
	12	958	20	15.9	3.58	—	—	—	-278.1	-62.5	-278.1	-62.5
	9	958	20	0.	0.	—	—	—	-81.9	-18.4	-81.9	-18.4
EXTERNALLY BLOWN FLAP NOZZLE	38	0	0	16.1	3.62	4	647.5	145.5	-173.6	-39	473.9	106.5
	36	958	20	16.2	3.64	↓	1936.	435	-213.6	-48	1722.	387
	35	958	20	0.	0.	↓	1179.	265	-35.6	-8	1144.	257

FIGURE 1. INTERFERENCE LIFT DUE TO POWER ON WING IN PRESENCE OF NACELLES

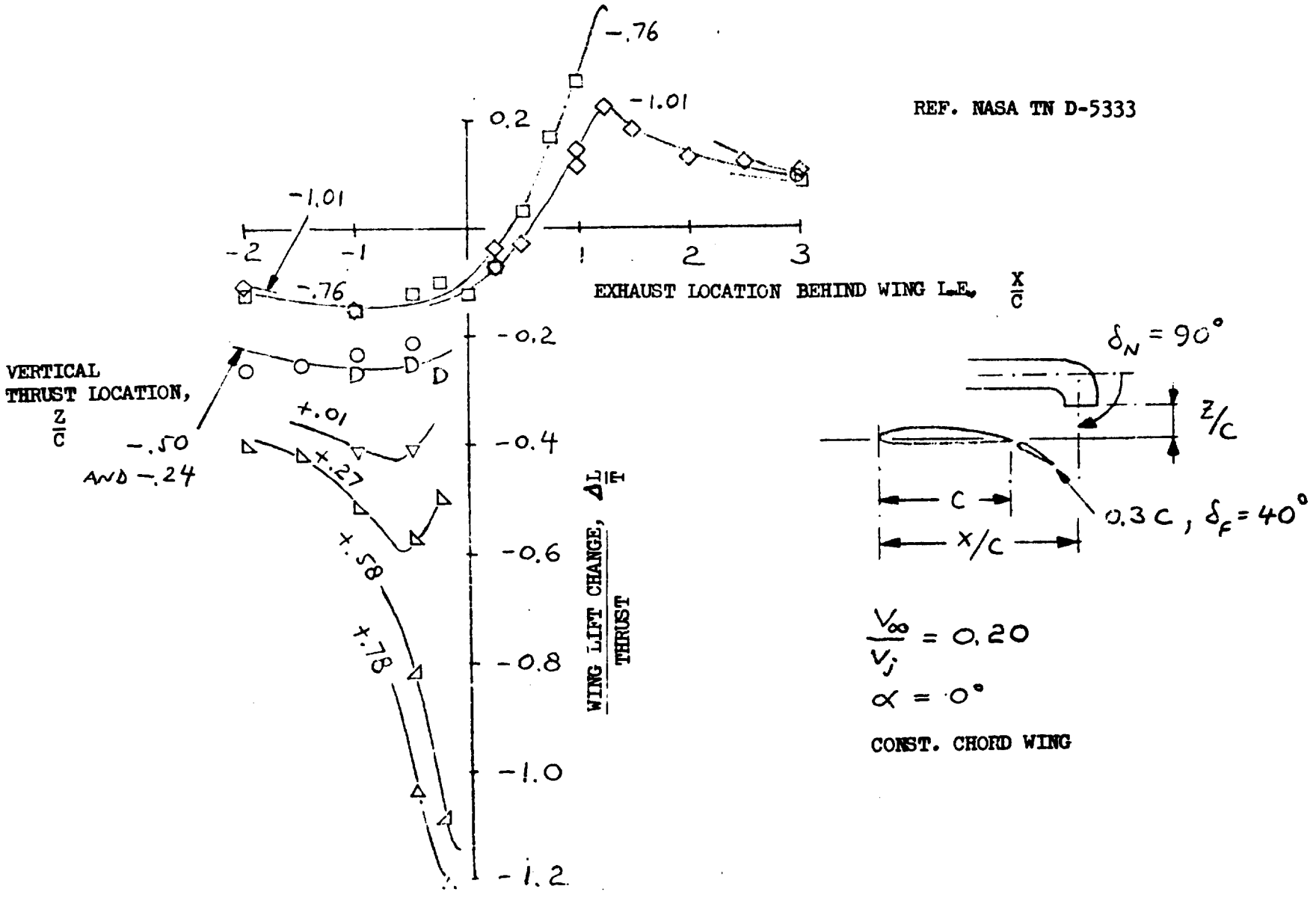

FIGURE 2. INTERFERENCE LIFT DUE TO POWER FOR VARIOUS FLAP DEFLECTIONS

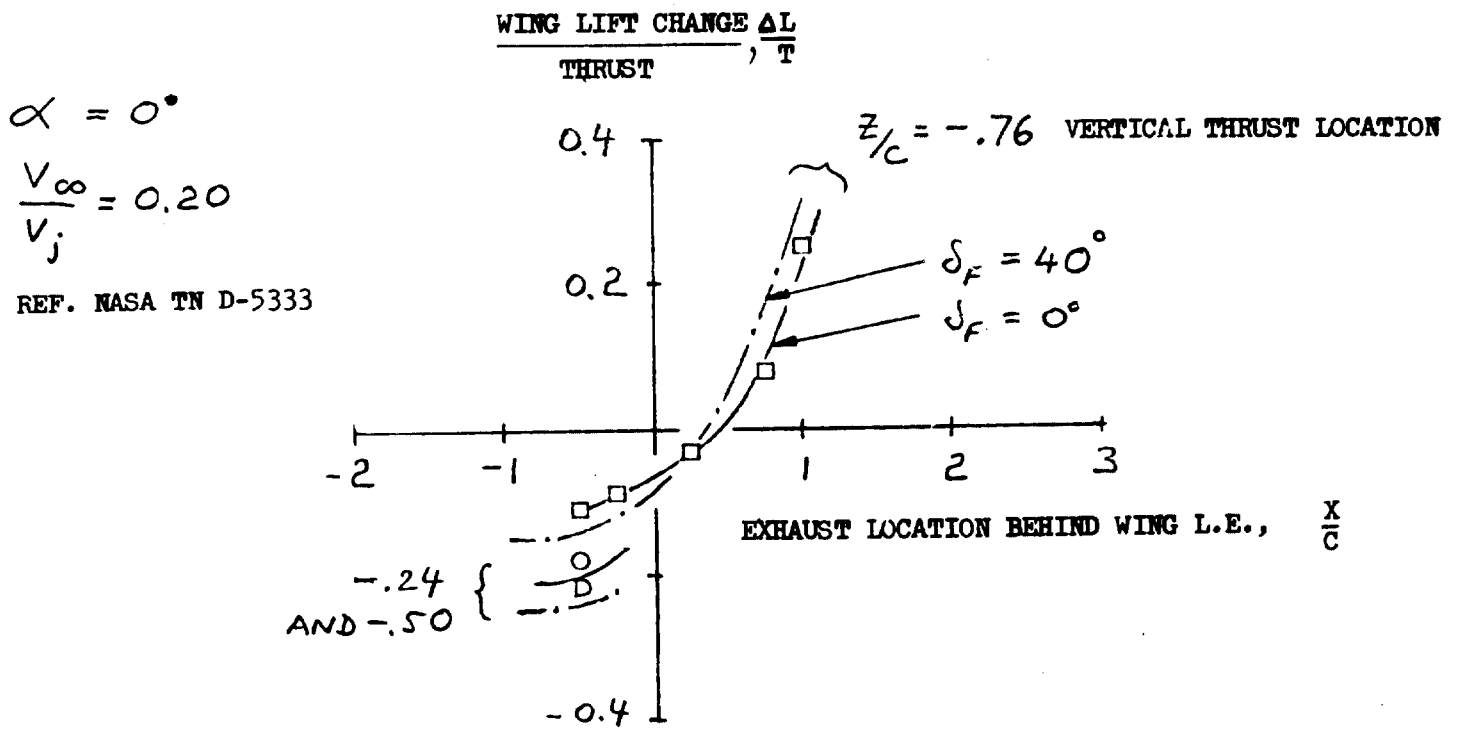

FIGURE 3. AIRCRAFT INTERFERENCE LIFT DUE TO POWER

$\frac{V_\infty}{V_j} = 0.2$, $\alpha = 0$ VERTICAL THRUST LOCATION Z/C = -0.60
(C = LOCAL CHORD)

REF. NASA TN D-7191

FLAP ANGLE

□ $\delta_F = 40°$

○ $\delta_F = 0°$

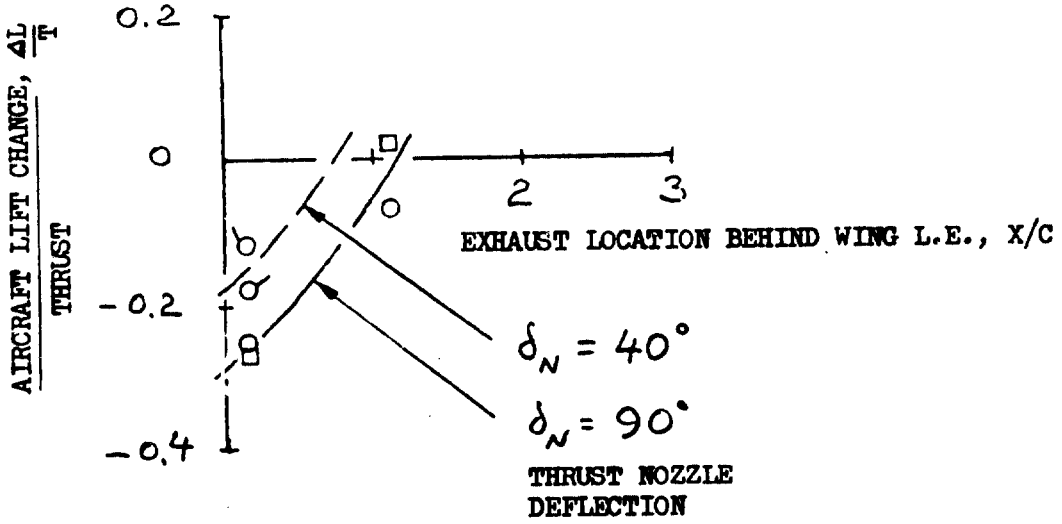

FIGURE 4. EFFECT OF SPEED ON INTERFERENCE LIFT DUE TO POWER

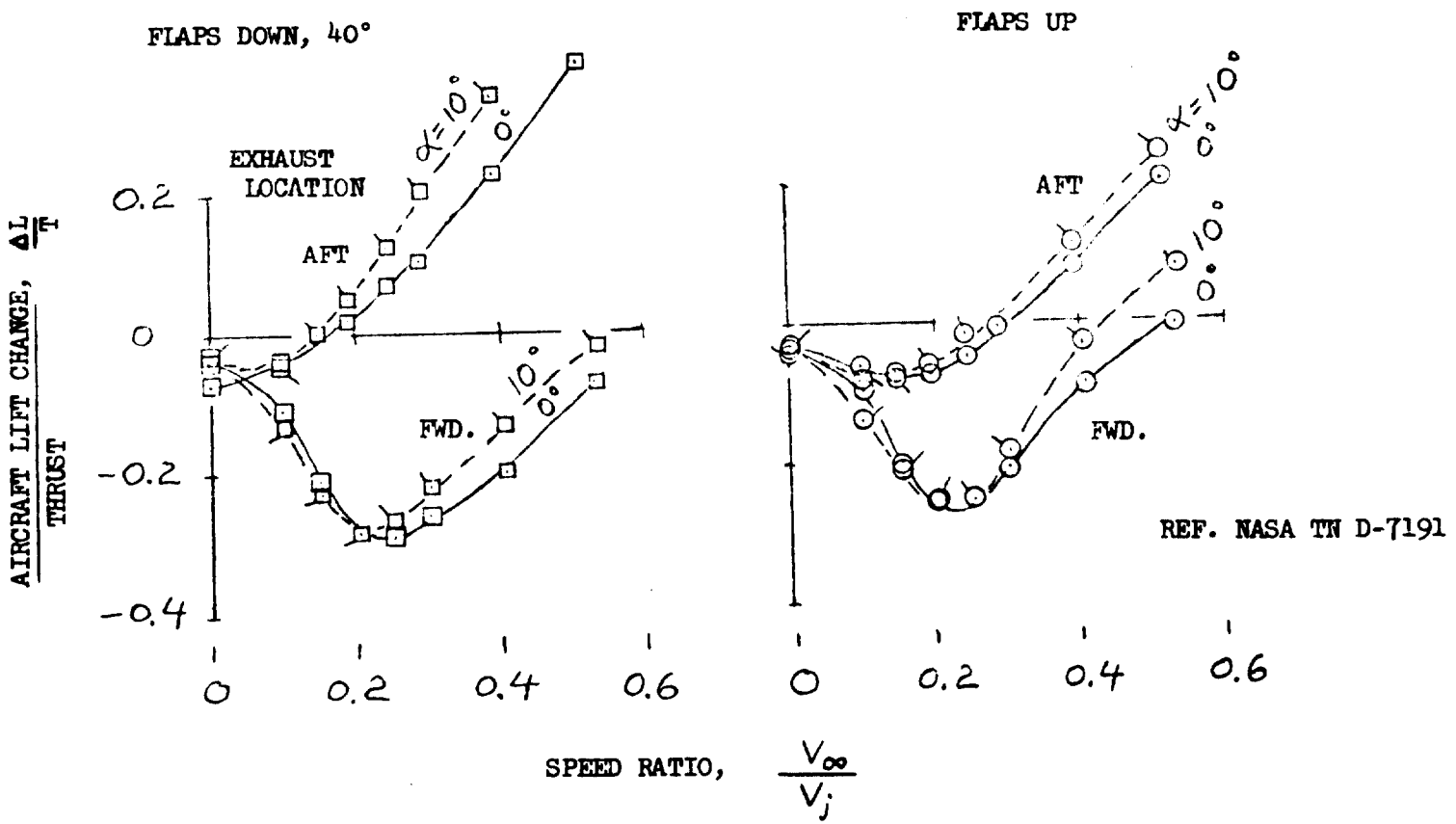

UNDERWING NOZZLES

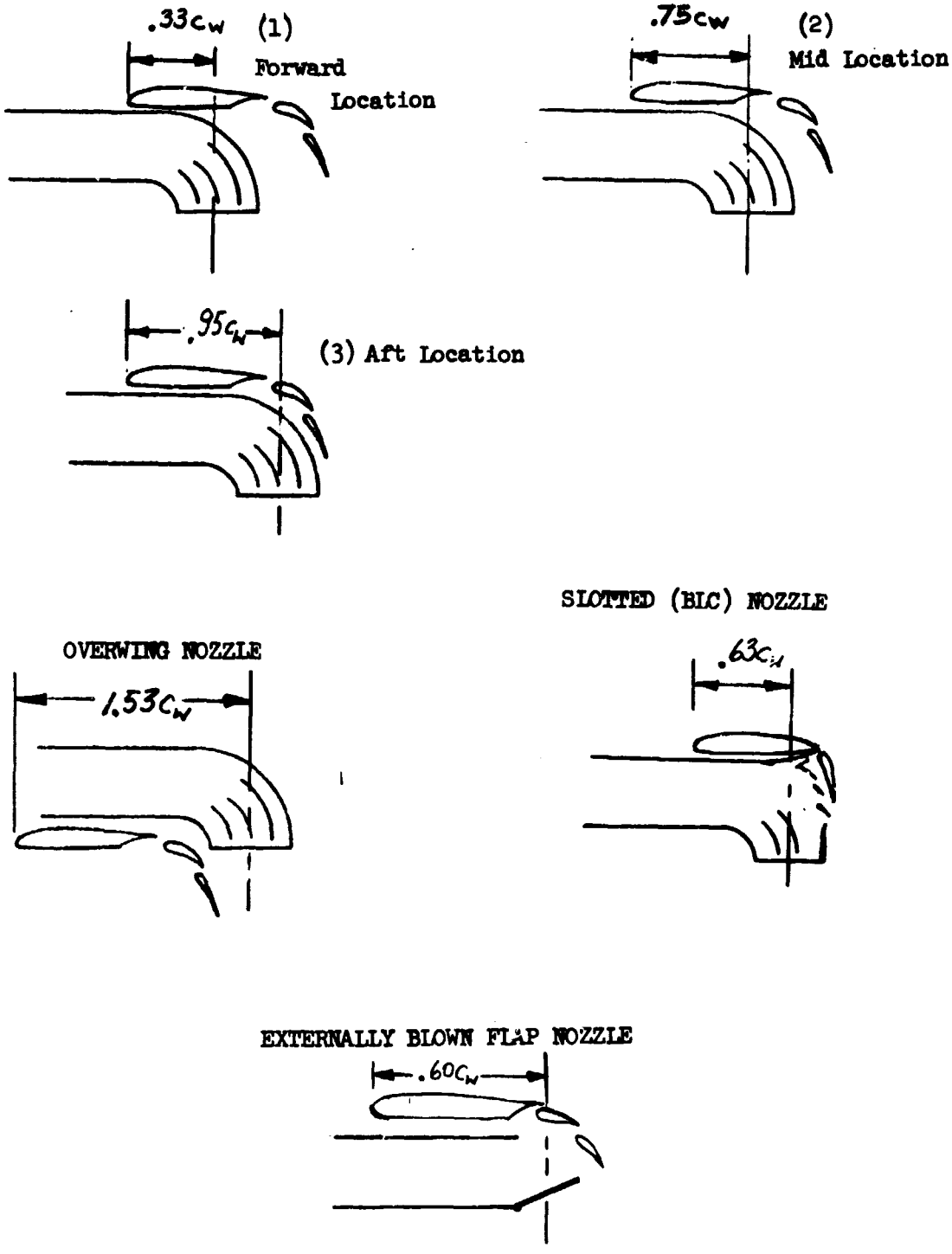

FIGURE 5. EJECTOR NOZZLES

FIGURE 6. MODEL INSTALLATION

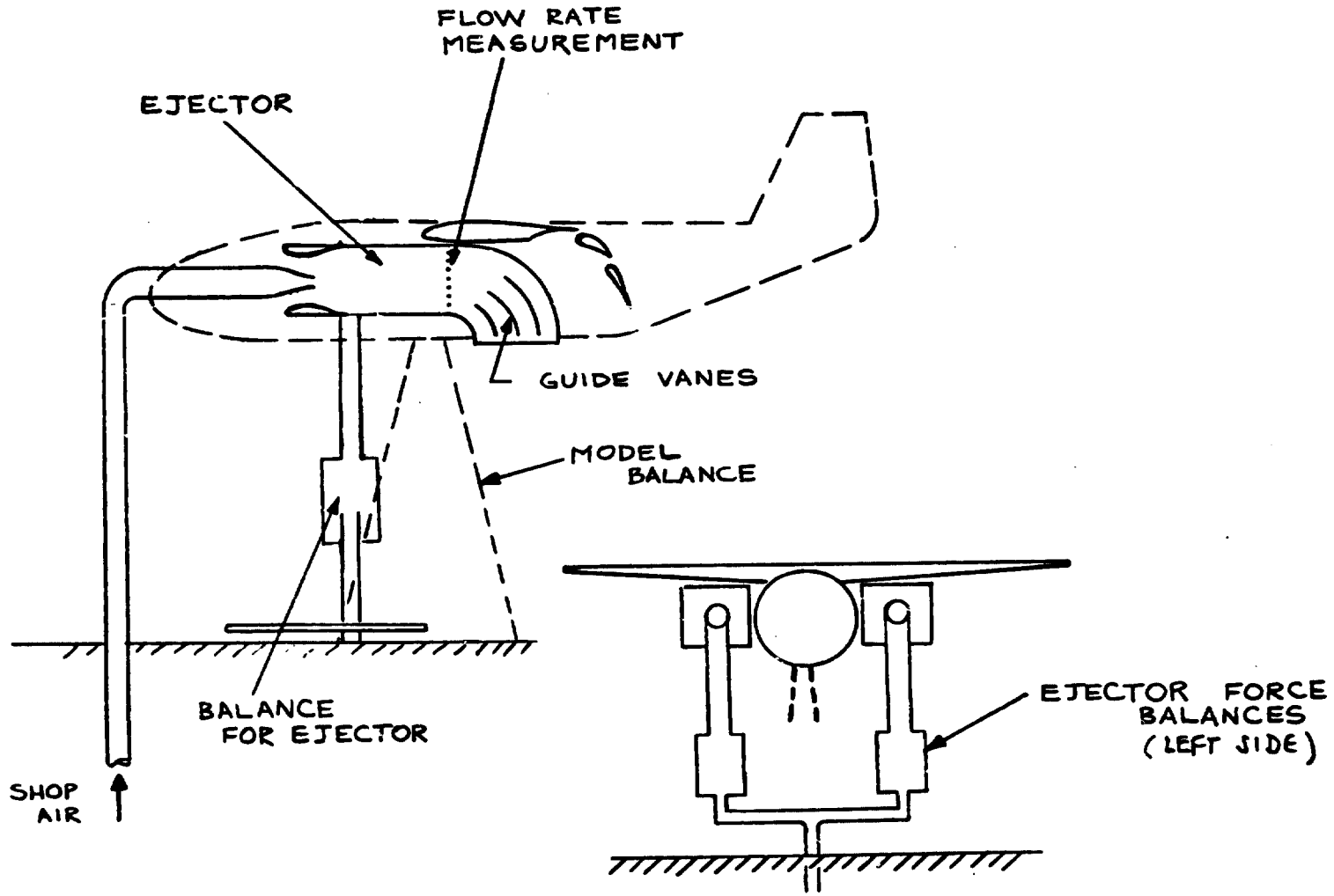

FIGURE 7. MODEL PLAN FORM WITH NACELLES IN FORWARD LOCATION

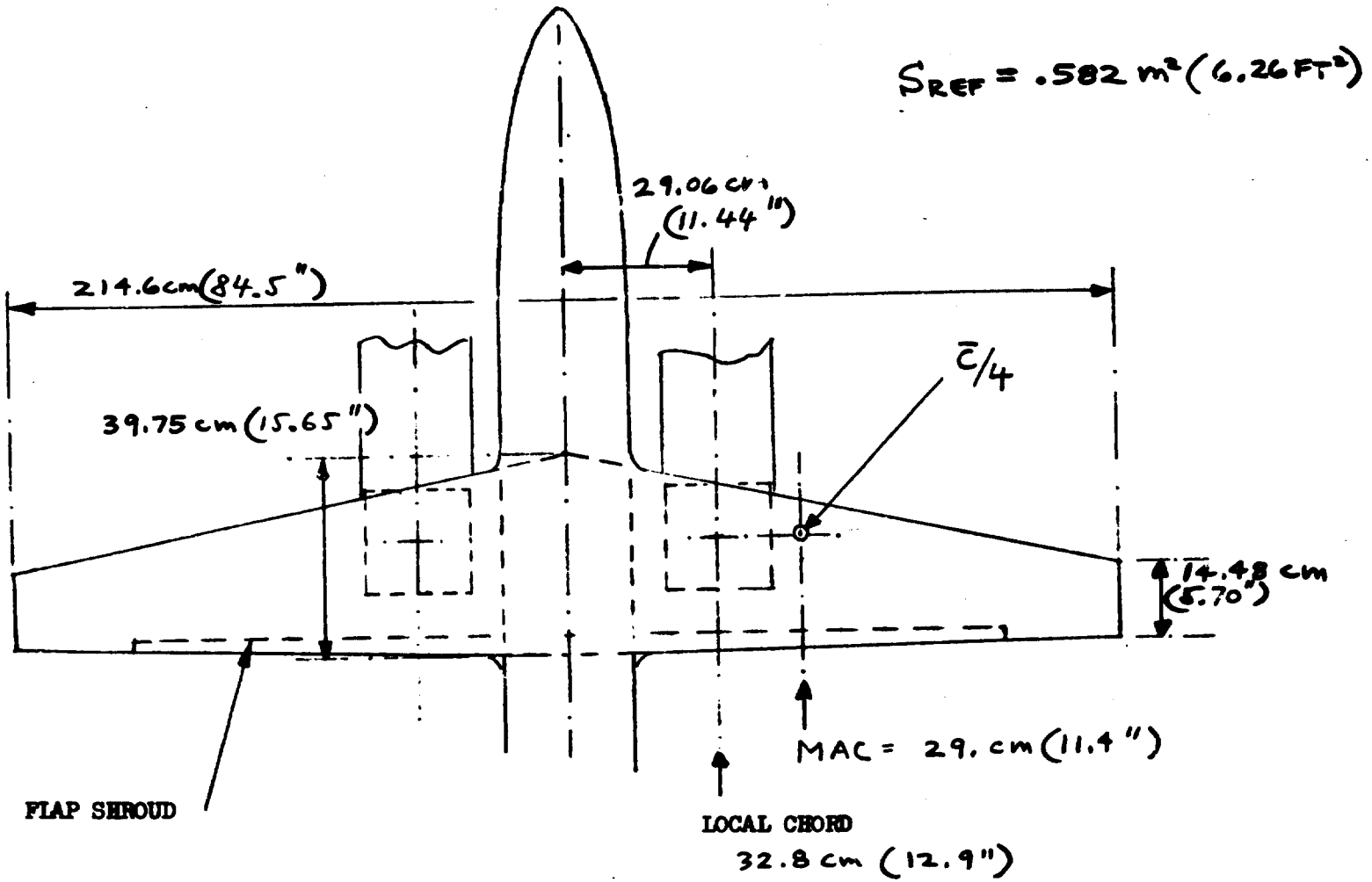

FIGURE 8. FLAP GEOMETRY

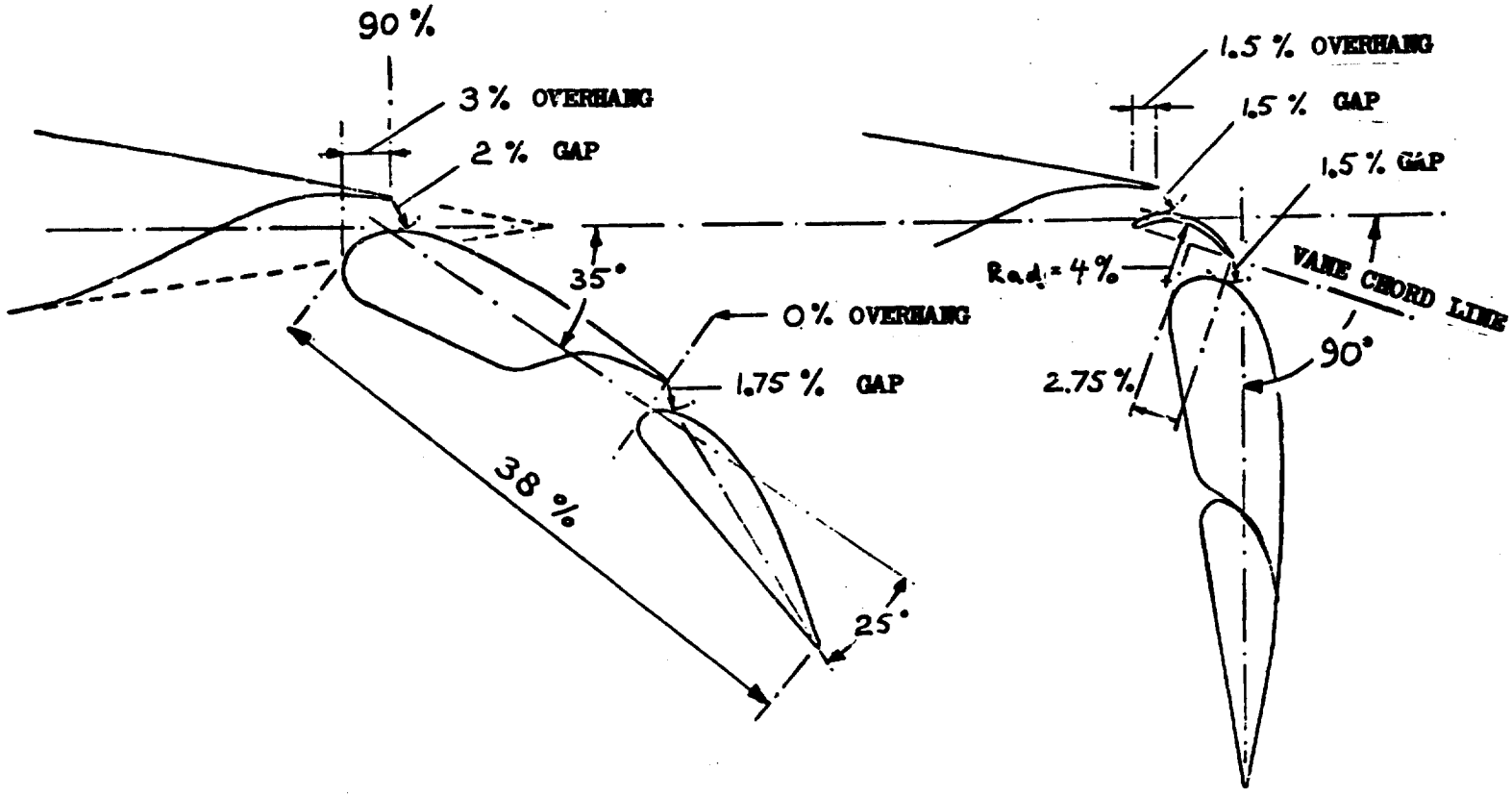

NOTE: ALL DIMENSIONS ARE IN PERCENT OF MAC.

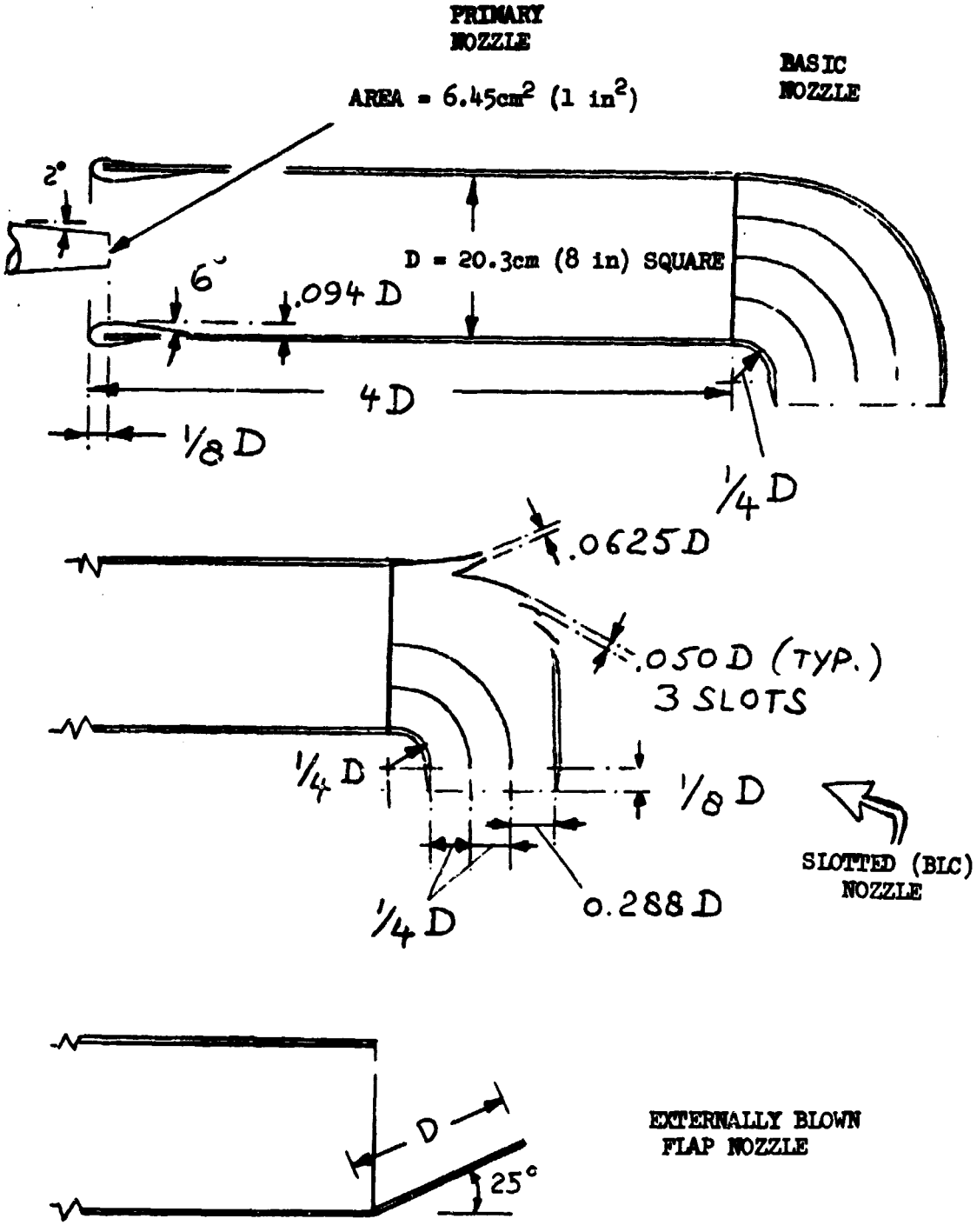

FIGURE 7. EJECTOR DETAILS

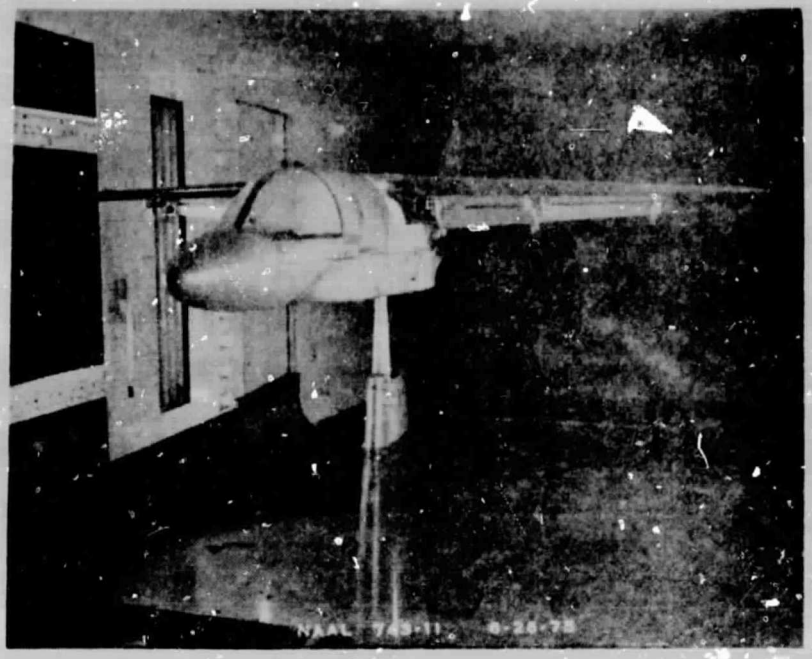

(a) MODEL ALONE

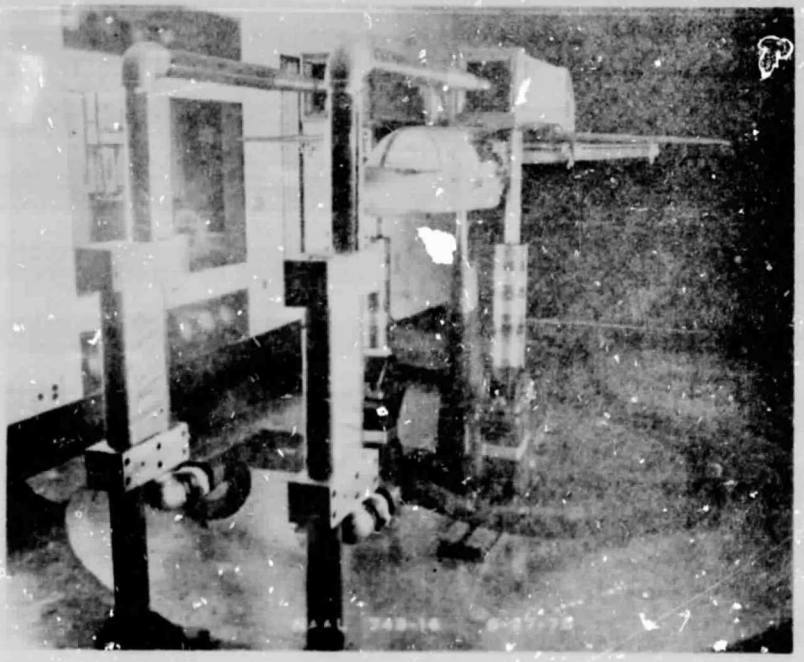

(b) MODEL + NACELLE
+ SHOP AIR SUPPLY

FIGURE 10. WIND TUNNEL INSTALLATION PHOTOGRAPH

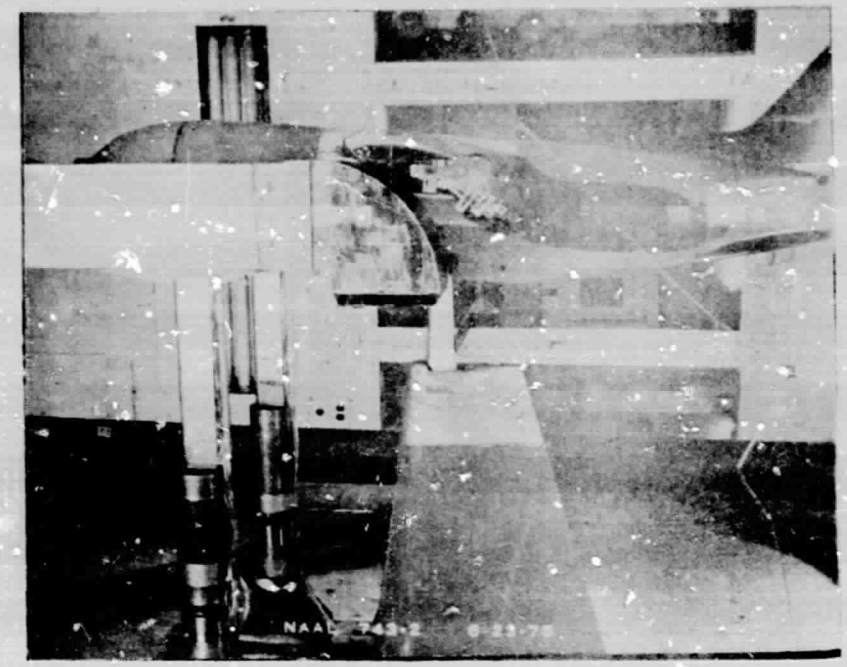

(a) Forward Underwing Nozzle

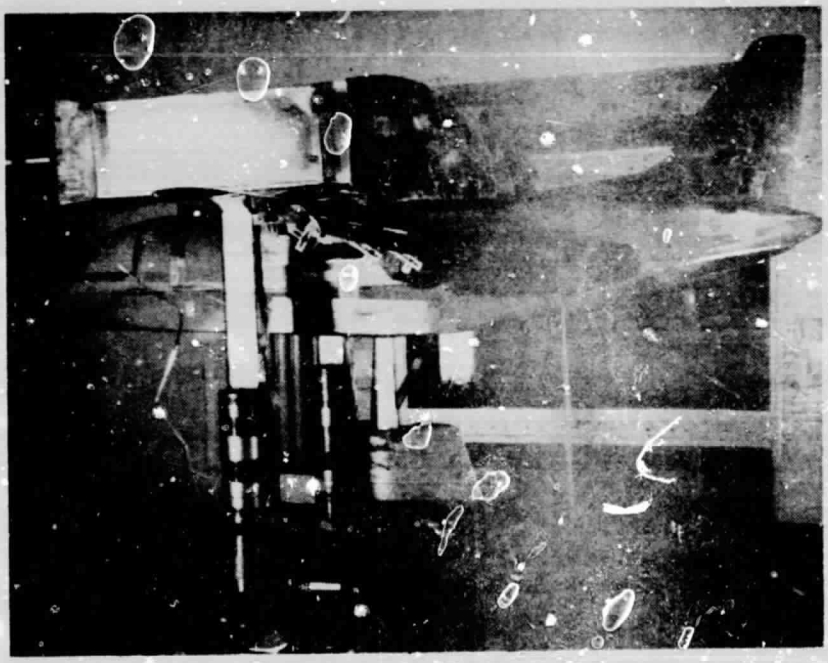

(b) Overwing Nozzle

FIGURE 11. NOZZLE LOCATION PHOTOGRAPH

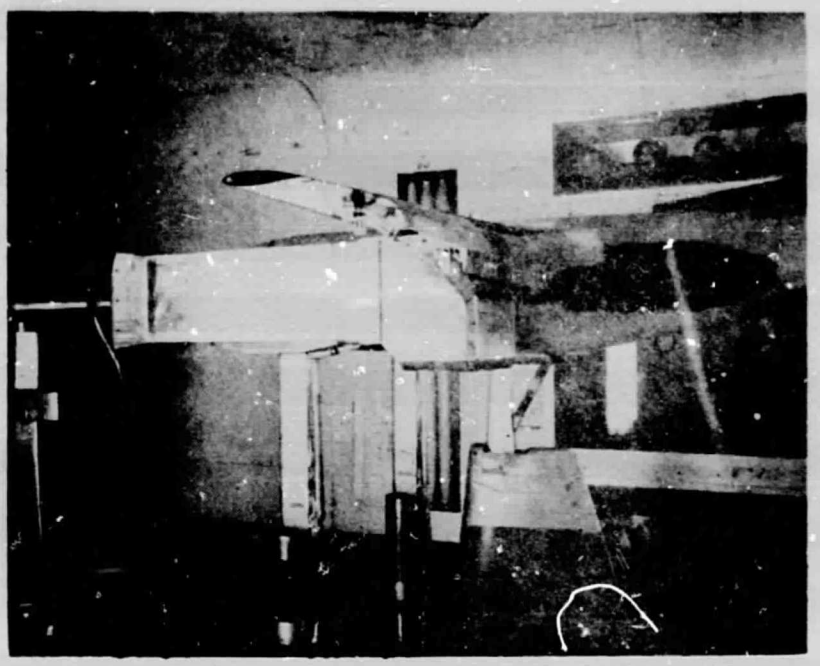

(a) Slotted (BLC) Nozzle

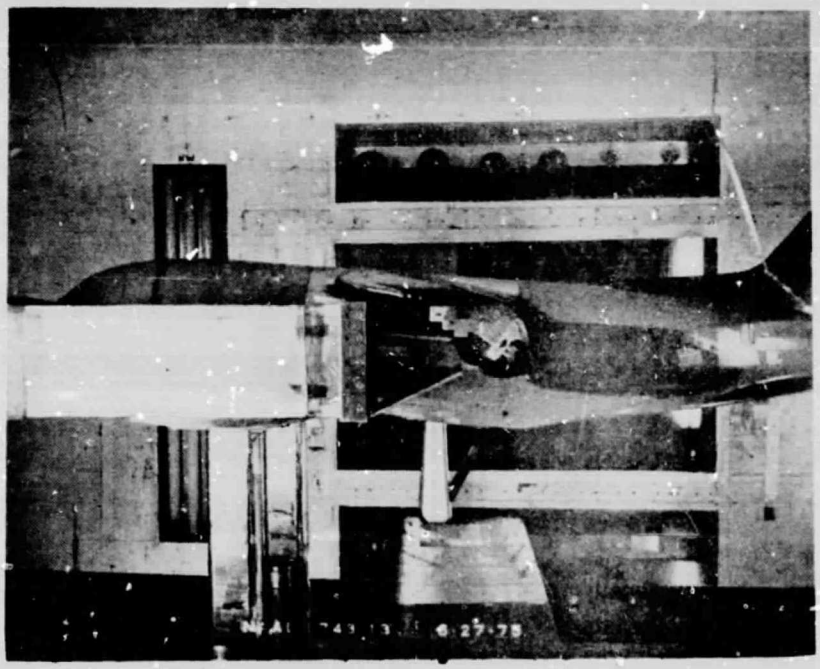

(b) Externally Blown Flap Nozzle

FIGURE 12. NOZZLE INSTALLATION PHOTOGRAPH

FIGURE 13. BASIC MODEL ALONE AND MODEL PLUS NOZZLE IN PRESENCE OF EACH OTHER

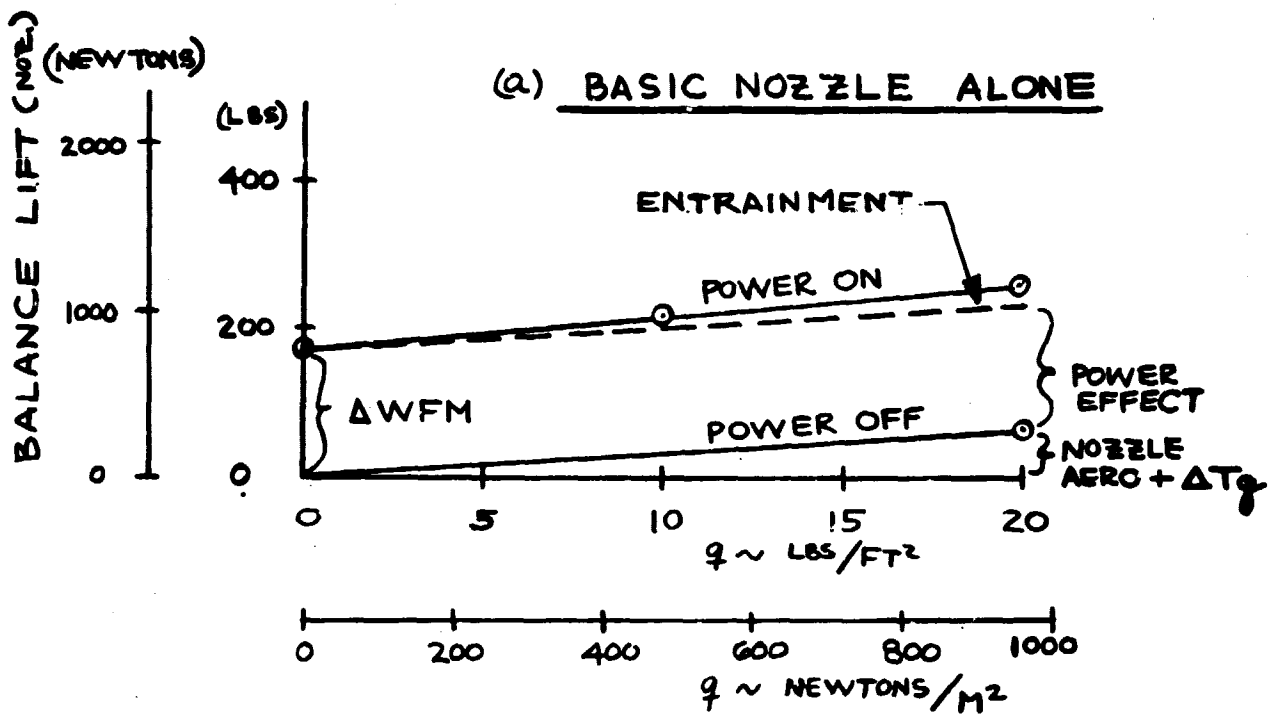

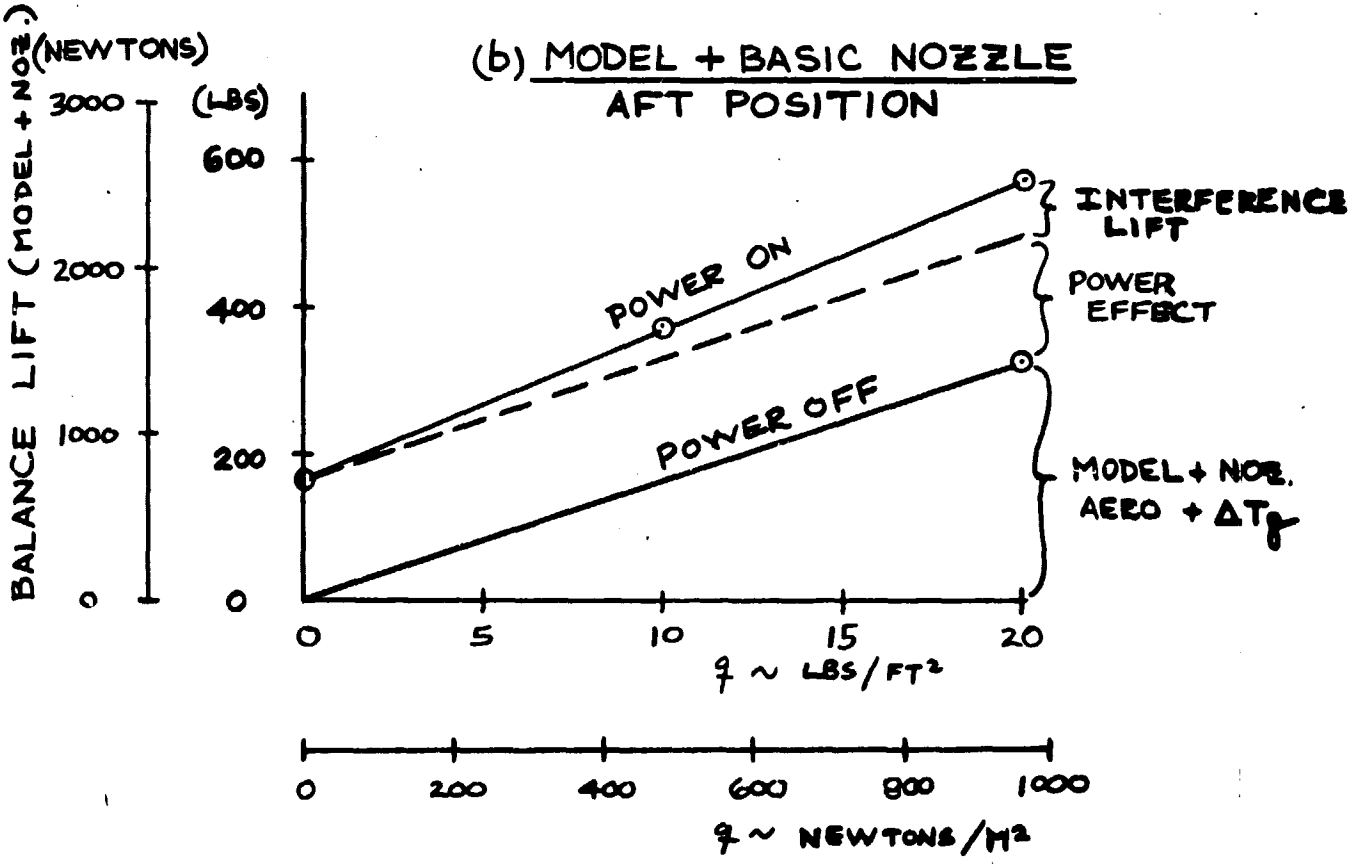

FIGURE 14. LIFT OF NACELLES IN PRESENCE OF WING AND BODY

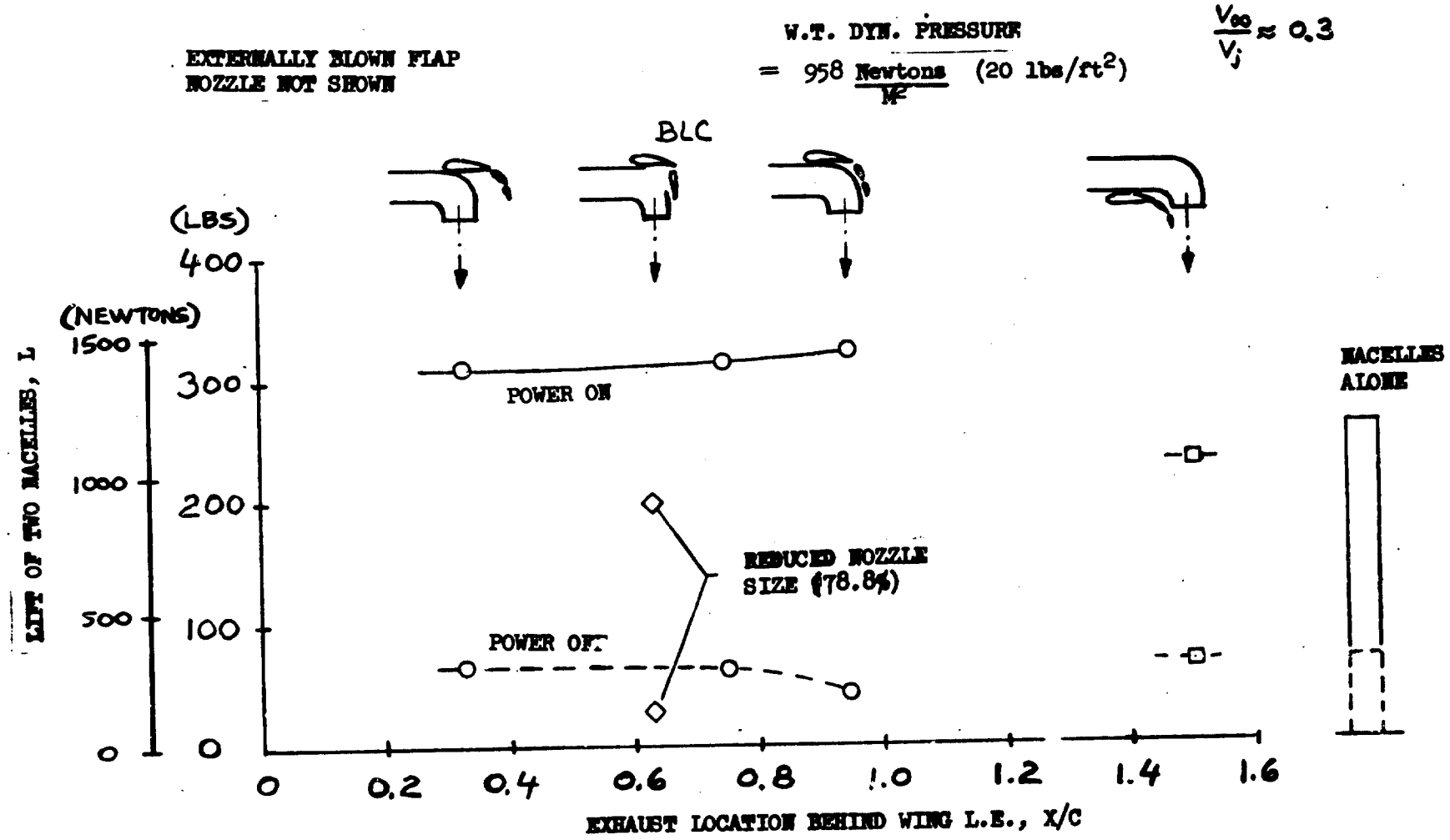

FIGURE 15. SCHEMATIC OF LOCATION OF NEGATIVE PRESSURE REGION

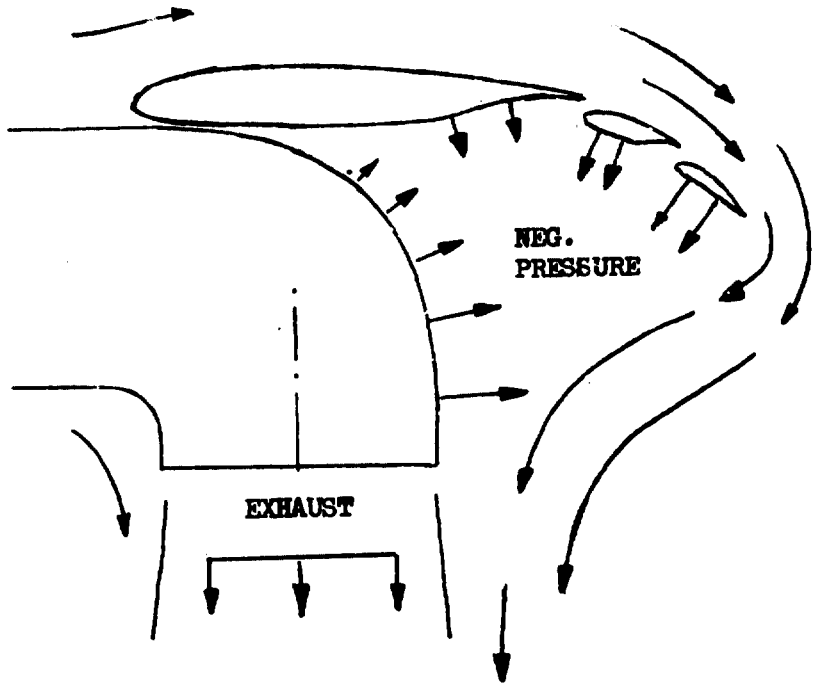

FIGURE 16. PRESSURES AT LOWER WING SURFACE

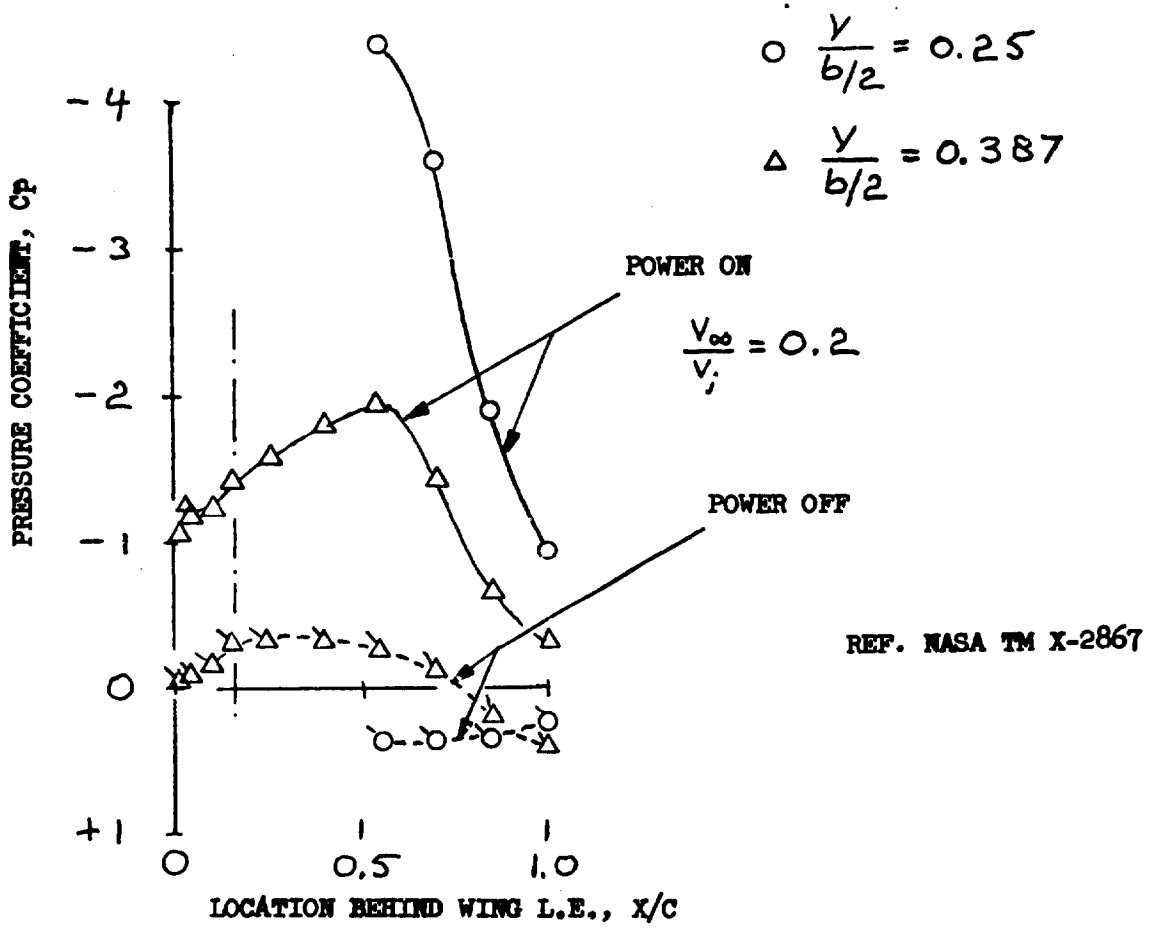

FIGURE 17. LIFT OF WING AND BODY IN PRESENCE OF NACELLES

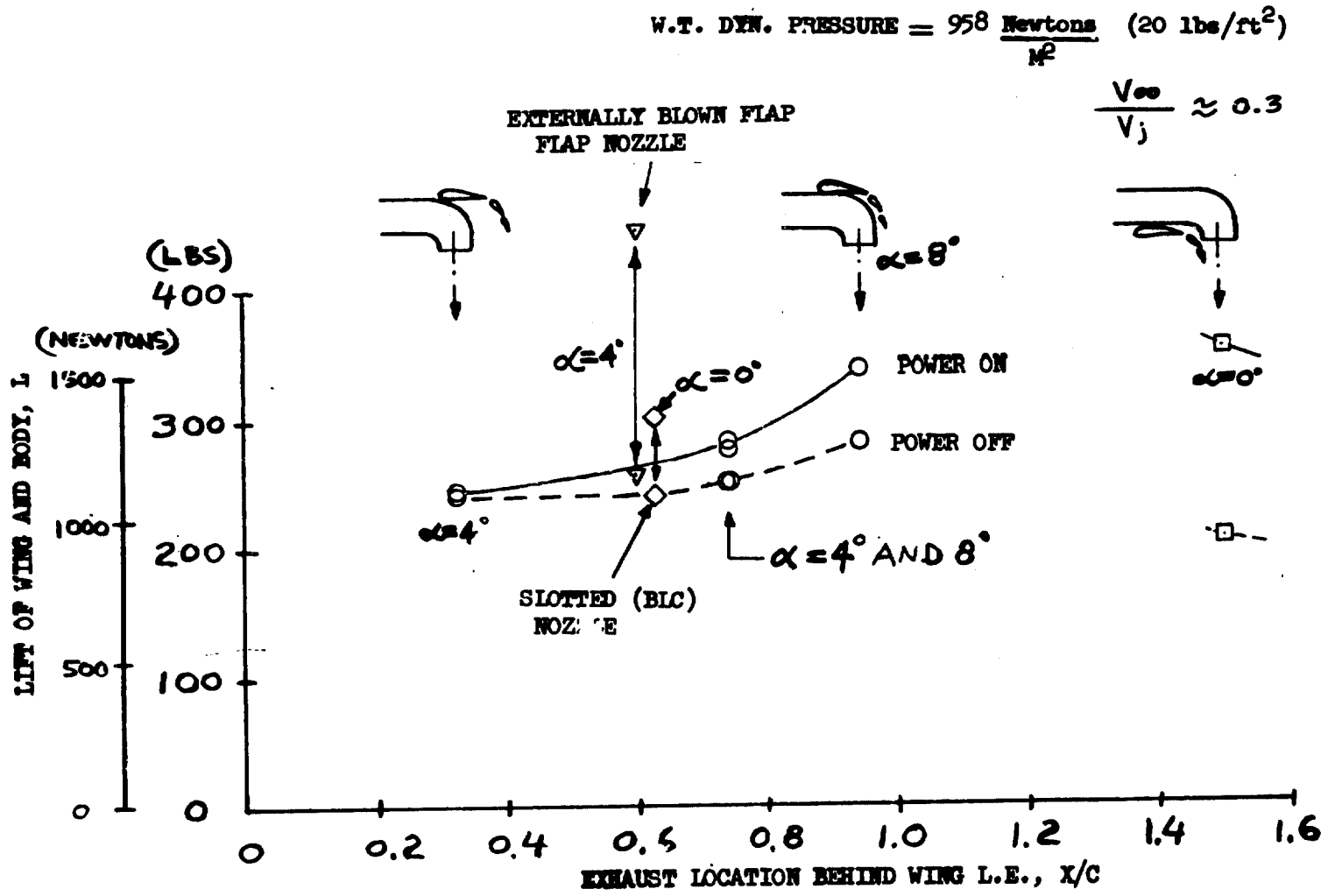

FIGURE 18. LIFT OF MODEL WITHOUT EJECTOR NACELLES

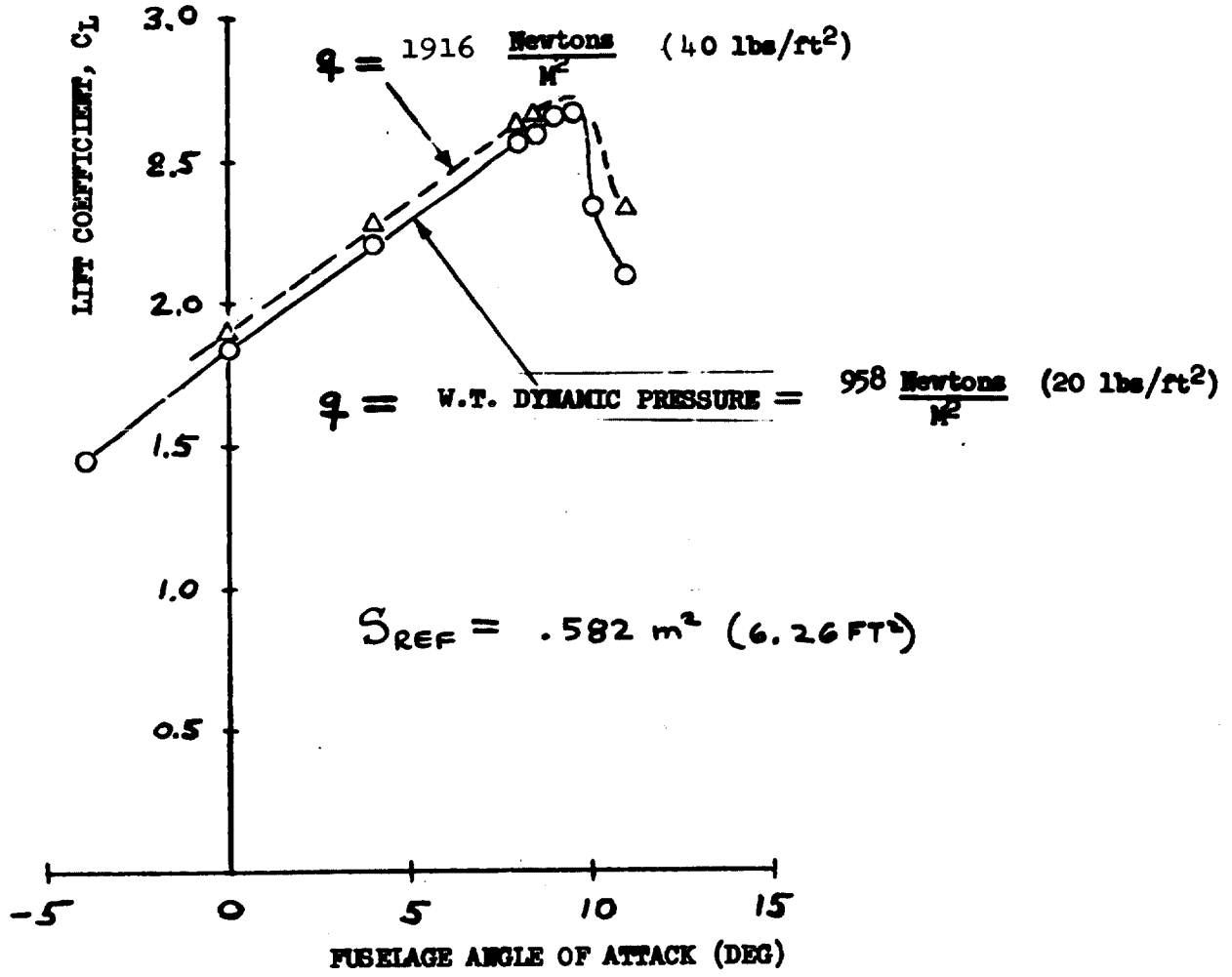

FIGURE 19. TOTAL LIFT OF WING, BODY, AND NACELLES

W. T. DYN. PRESSURE
$= 958 \frac{\text{Newtons}}{M^2}$ (20 lbs/ft^2)

$\frac{V_\infty}{V_j} \approx 0.3$

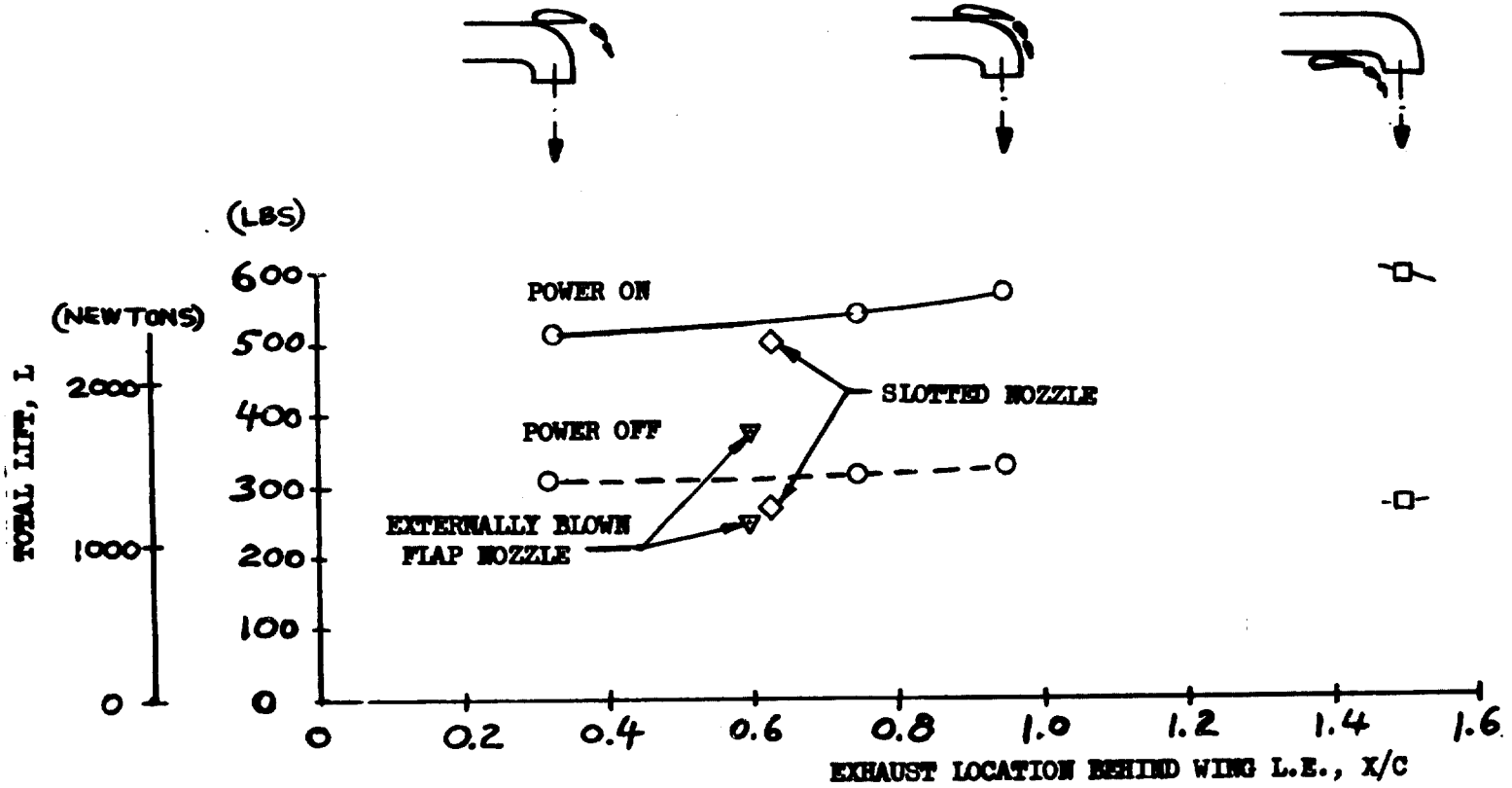

Figure 20. Change in Lift Due to Power for Various Nozzles

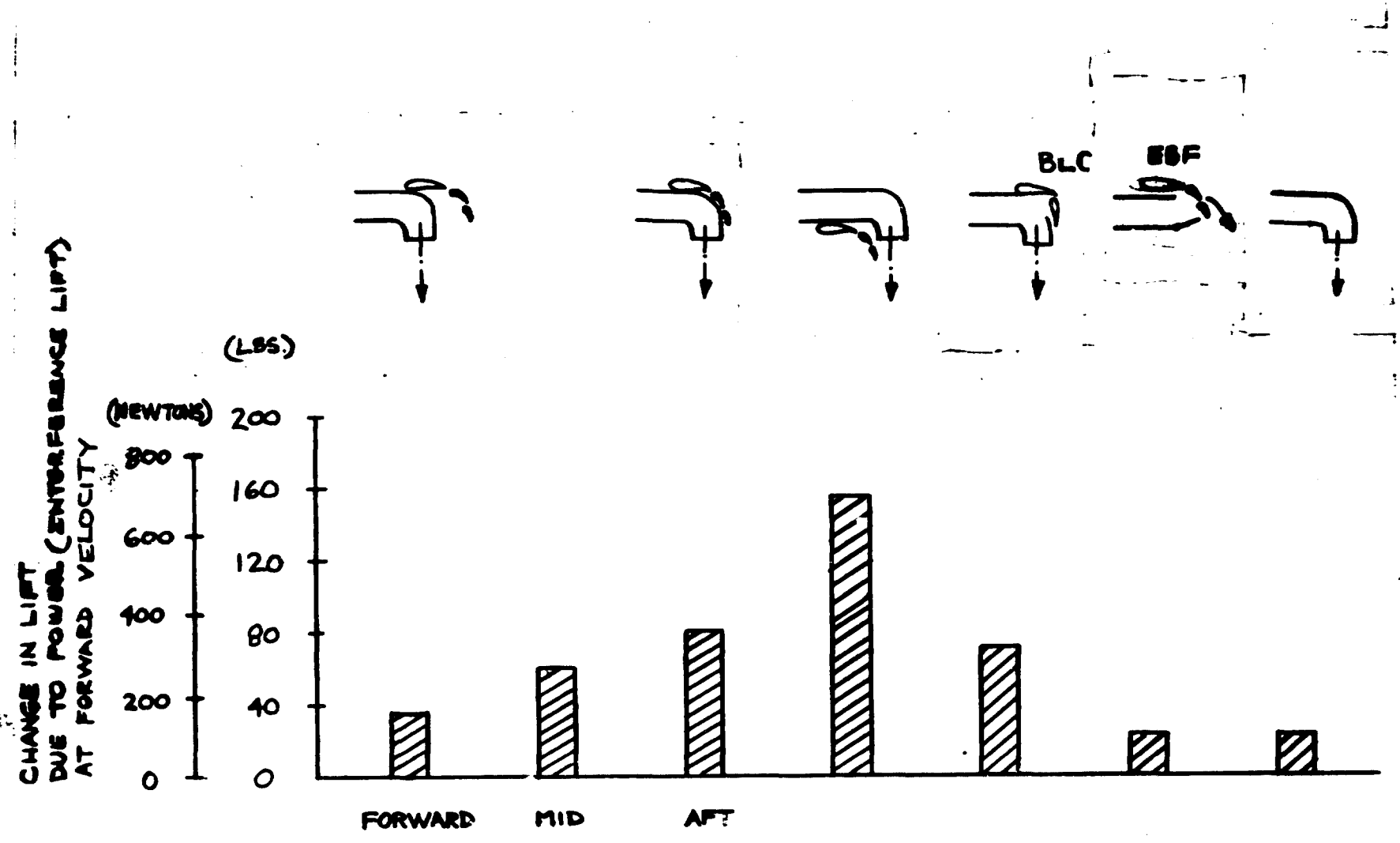

Figure 21. Wing Lift Change in Presence of Nacelles

W.T. Dyn. Pressure = 958 $\frac{\text{Newtons}}{\text{M}^2}$ (20 lbs/ft^2)

$\frac{V_{\infty}}{V_j} \approx$ [illegible]